Time of Flight Secondary Ion Mass Spectrometry imaging for precise localization of zirconium-labelled trastuzumab in xenograft cancer tumour

Microchemical Journal 181 (2022) 107860

Contents lists available at ScienceDirect

Microchemical Journal

journal homepage: www.elsevier.com/locate/microc

Time of Flight Secondary Ion Mass Spectrometry imaging for precise localization of zirconium-labelled trastuzumab in xenograft cancer tumour tissues

Florent Penen [a], René Raavé [b], Annemarie Kip [b], Sandra Heskamp [b], Per Malmberg [a,*]

[a] Department of Chemistry and Chemical Engineering, Chalmers University of Technology, Gothenburg SE-412 96, Sweden
[b] Department of Medical Imaging, Nuclear Medicine, Radboud University Medical Center, Nijmegen, The Netherlands

ARTICLE INFO

Keywords:
Mass spectrometry imaging
Secondary ion mass spectrometry SIMS
Zirconium-89

ABSTRACT

The human epidermal growth factor receptor 2 (HER2) specific radiotracer zirconium-Desferrioxamine(DFO)-trastuzumab was visualized *ex-vivo* by Time of Flight Secondary Ion Mass Spectrometry (ToF-SIMS) imaging in ovarian and breast cancer xenograft tumor sections. Heterogeneous spatial distribution of [$^{90}Zr^{+}$] ions reflected the heterogeneous localization of trastuzumab, observed in parallel by immunohistochemistry staining in $HER2^{+}$ tumors. Our results show that ToF-SIMS imaging is a quick and sensitive technique to image zirconium labelled biologics at microscale in tissues.

1. Introduction

Immuno-positron emission tomography (ImmunoPET) can play a pivotal role in the molecular characterization of tumours and evaluation of novel therapeutic agents. ImmunoPET with zirconium-89 (^{89}Zr) labelled antibodies can reveal safety issues of new monoclonal antibodies such a maldistribution in target and non-target tissues [1]. However, the spatial resolution of clinical PET systems is only ~ 5 mm, therefore detailed visualization of heterogeneity within tissues is limited. *Ex vivo* immunohistochemical analysis of tissues can provide information on the distribution of antibodies at the level of tissues. However, no methods are available to visualize the distribution of antibodies at (sub)cellular levels without the need of additional immunohistochemical analyses. Here, the use of Time of Flight Secondary Ion Mass Spectrometry (ToF-SIMS) imaging for *ex vivo* localization of zirconium (Zr) resulting from a model antibody conjugate, Zr-Desferrioxamine(DFO)-trastuzumab (Fig. 1), from tissue to (sub) cellular resolution is described.

ToF-SIMS is a technique to study the surface molecular composition of material [2–4], geological [5–7] and biological samples [8–10]. It has successfully been used to image the distribution of metallodrugs [11,12] and gadolinium-based magnetic resonance imaging (MRI) contrast agents [13] at the tissue and cellular level, demonstrating its potential to *ex vivo* determine the distribution of metal-labelled compounds. With a detection limit in the order of ppm and a submicron lateral resolution, ToF-SIMS imaging provides isotopic, elemental and molecular maps of a tissue surface. Sample preparation is critical to preserve the native structure and chemistry of cells and tissues and to prevent release of Zr ions from Zr-DFO-trastuzumab conjugates is of critical importance. Freeze-dried and frozen-hydrated preparations are considered the best way to analyse biological samples using ToF-SIMS imaging [14,15] and allows analysis of biological non-fixed tissues without washing and the use of probes and or antibodies, avoiding changes or leakage in the distribution Zr ions resulting from Zr-DFO-trastuzumab.

In this study, the human human epidermal growth factor receptor 2 (HER2) high expressing ($HER2^{+}$) SKOV-3 and low HER2 expressing ($HER2^{-}$) MDA-MB-231 cells were cultured *in vitro* and inoculated subcutaneously in nude mice. Once the tumours reached a size of 0.4–0.5 mm^3, mice were injected with 300 μg Zr-DFO-trastuzumab. After 3 days, mice were sacrificed, and tumours were collected and snap frozen. Tumour sections were prepared for ToF-SIMS and immunohistochemistry (IHC) analysis (see supplementary information for more details). The Zr-DFO-trastuzumab localization was compared using the two imaging techniques (see Fig. 2 for schematic overview).

* Corresponding author.
E-mail address: malmper@chalmers.se (P. Malmberg).

https://doi.org/10.1016/j.microc.2022.107860
Received 27 June 2022; Received in revised form 1 August 2022; Accepted 3 August 2022
Available online 6 August 2022

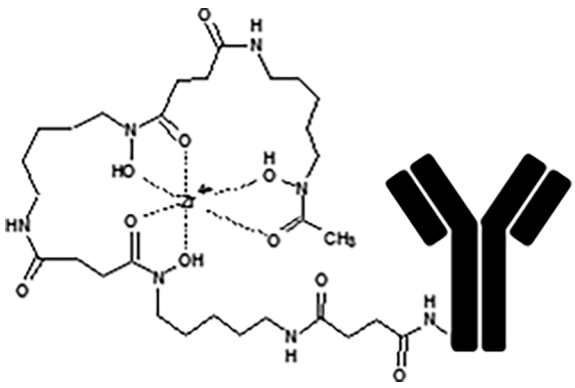

Fig. 1. Example of the Zr-DFO-trastuzumab complex.

2. Materials and methods

2.1. Zr labeling of conjugate

DFO-*N*-SucDf-trastuzumab (DFO-trastuzumab) was provided and by UMCG, Groningen, the Netherlands). Trastuzumab was conjugated with *N*-SucDf and verified by the methods according to the procedures described by Dijkers et al. [16]. DFO-trastuzumab was labeled with a 5 times molar excess of non-radioactive zirconium (kindly obtained from B.V. Cyclotron Amsterdam, the Netherlands). In short, Zr(IV) in 80 μl oxalic acid was diluted with 160 μl and the pH was neutralized with 36 μl Na_2CO_3 and 500 μl 0.5 M 4-(2-hydroxyethyl)-1-piperazineethanesulfonic acid (HEPES, pH 7) buffer. The neutralized Zr(IV) solution was incubated with 1 mg DFO-trastuzumab for 1 h at RT. Free Zr(IV) was removed by dialysis at 20,000 MWCO to PBS (pH 7.4). To verify the complexation of Zr(IV) with DFO-trastuzumab a labeling with [^{89}Zr]Zr(IV) was performed. When the labeling with non-radioactive Zr (IV) was successful, the subsequent labeling with radioactive [^{89}Zr]Zr (IV) would not be possible. A similar procedure as for non-radioactive labeling was performed, but with 0.1 Mbq [^{89}Zr]Zr(IV) (PerkinElmer, B.V. Cyclotron, Amsterdam, the Netherlands) instead of Zr(IV), to 10 μg Zr-DFO-trastuzumab. The radiolabeling was evaluated with instant-Thin Layer Chromatography with silica gel impregnated strips (iTLC-SG). The [^{89}Zr]Zr(IV) radiolabeling was <1 %.

2.2. Cell culture

The human HER2 high expressing (HER2$^+$) cell line SKOV-3 (HTB-77, ATCC) and the HER2 low expressing (HER2$^-$) cell line MDA-MB-231 (HTB-26, ATCC) were cultured in RPMI-1640 (GIBCO, ThermoFisher Scientific, Waltham, MA, USA) media supplemented with 2 mM glutamine (GIBCO) and 10 % fetal calf serum (Sigma-Aldrich Chemie BV), at 37 °C in a humidified atmosphere with 5 % CO_2. At 80–90 % confluency, cells were dissociated using 0.05 % trypsin (w/v) in 0.53 mM EDTA (Life Technologies) and maintained as proliferating cultures. Mycoplasma contamination was evaluated every-four months using a MycoAlert™ mycoplasma detection kit (Lonza, Basel, Switzerland). After thawing, cells remained in culture for a maximum of six months.

2.3. Animals

The Dutch central committee on animal research and the local ethical committee on animal research of the Radboud University approved this study under protocol 2015–0071. All animal experiments were performed according to the institutional guidelines. Upon arrival, 6–8 weeks old female BALB/cAnNRj-Foxn1^{nu}/Foxn1^{nu} mice (Janvier Labs, France) were randomly tattooed for identification and were acclimatized for ≥ 4 days before any experimental procedure. Mice had unlimited access to food and water and were maintained with 3 mice per cage in a controlled environment (22 ± 1 °C, 55 ± 10 % humidity, 12 h dark/light cycle). Cages were weekly replaced by clean cages. Mice were assessed daily for welfare and the tumor size was measured twice a week after tumor inoculation. Mice were randomly allocated to the experimental groups according to a random sequence generator and the biotechnicians performing the experiments were blinded. Tumors were inoculated by subcutaneous (s.c.) injection of 5 · 10^6 SKOV-3 or MDA-MB-231 cells mixed 2:1 or 1:1 in Matrigel (BD Biosciences; Pharmingen), respectively. Experiments started when tumors reached a size of 0.4 – 0.5 mm^3.

2.4. In vivo study

A mouse bearing HER2$^+$ SKOV3 tumor and a mouse bearing a HER2$^-$ MDA-MB-231 tumor were injected with 300 μg Zr-DFO-trastuzumab. One mouse bearing a HER2$^+$ SKOV3 tumor was injected with non-labeled trastuzumab. Three days after injection, mice were euthanized by CO_2 asphyxiation and the tumors were collected, snap frozen in isopentane on dry-ice (-80 °C) and stored at −80 °C. For ToF-SIMS analysis 20 μm sections were cut and immobilized on MALDI imaging glass slides with conductive ITO coating (Bruker Daltonik, Bremen, Germany). For reference stainings, 5 μm sections were cut and immobilized on superfrost glass slides. Frozen sections were stored at −80 °C until further processing.

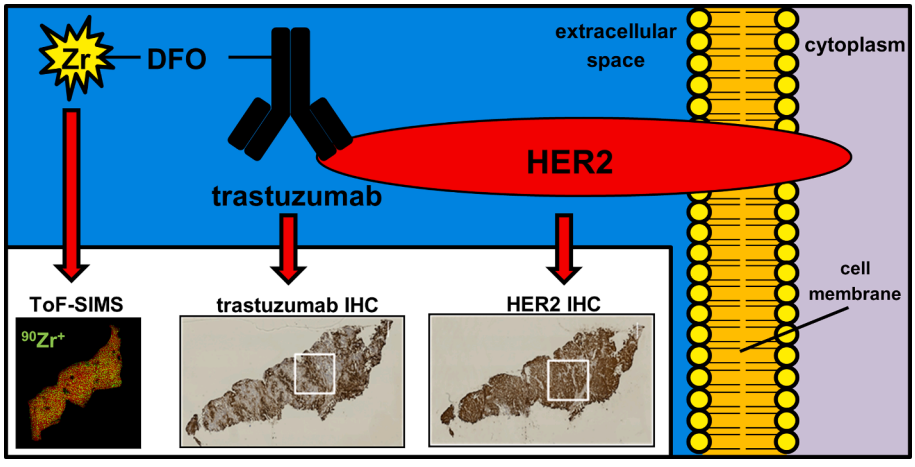

Fig. 2. Schematic overview of the methods used to detect Zr-DFO-trastuzumab. Zirconium-90 was visualized using ToF-SIMS. Sections from the same tumor were stained for presence of trastuzumab (trastuzumab IHC) and for presence of HER2 (HER2 IHC).

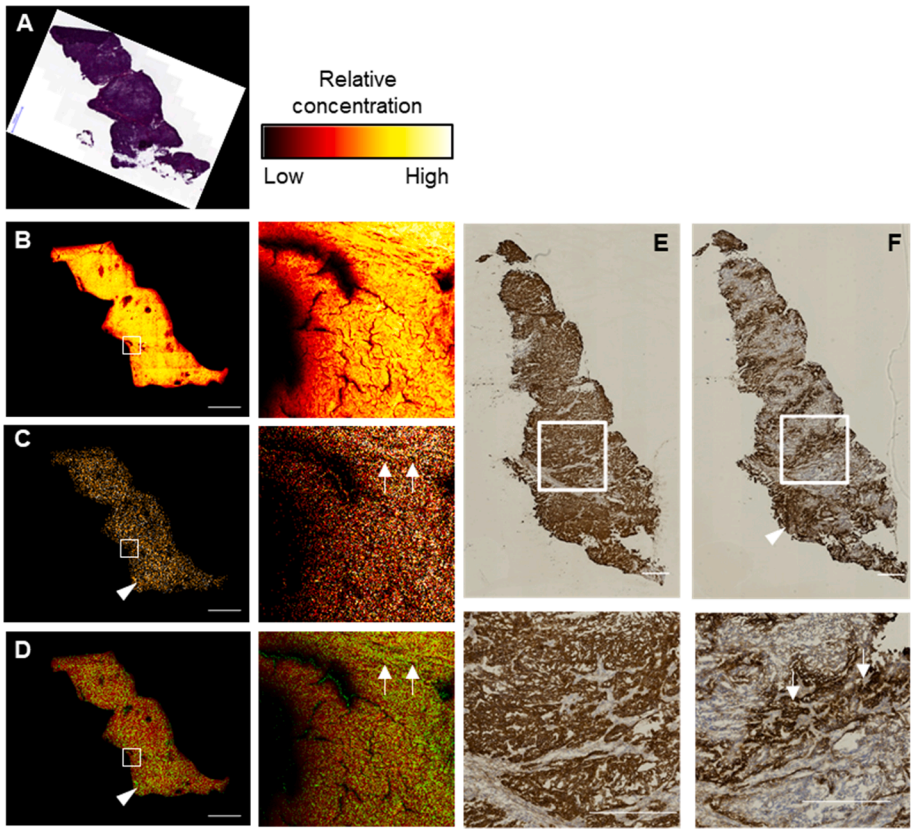

Fig 3. Zirconium spatial distribution in a section of $HER2^{+}$ xenograft tumour in a mouse injected with 300 μg of Zr-DFO-trastuzumab. (A) Haemotoxylin and eosin stained consecutive section. TOF-SIMS large scan mapping and corresponding close-up of (B) $[C_5H_{15}PO_4N]^{+}$ fragment (*m/z* 184.02), (C) $^{90}Zr^{+}$ (*m/z* 89.90) as well as (D) overlay of $[C_5H_{15}PO_4N]^{+}$ fragment and $^{90}Zr^{+}$ in red and green colour, respectively. Scale bar = 1 mm, close-up field of view = 500x500 μm^2. White arrows show regions rich in Zr. Sections were stained for for HER2 expression (E) and trastuzumab presence (F) with enlargement below the images with the scale bar representing 500 μm. (For interpretation of the references to colour in this figure legend, the reader is referred to the web version of this article.)

2.5. Immunohistochemistry

HER2 expression was determined by incubating the frozen sections with rabbit-a-human HER2 (DAKO, 500 times diluted in PBS) for 1 h at RT after fixation in aceton. After washing with PBS, the sections were incubated with goat-a-rabbit-biotin (Vector, 400 times diluted in PBS) for 30 min at RT, and subsequently incubated with an avidin–biotin complex (Vectastain ABC HRP kit, Vector) for 30 min at RT and a Bright DAB (Immunologic) with hematoxylin as counterstain. In vivo injected trastuzumab was stained on the tumor sections by incubating with goat-a-human-peroxidase (Abcam, 200 times diluted in PBS) for 1 h at RT and visualized using Bright DAB with hematoxylin as counterstain. Hematoxylin and Eosin (H&E) stainings were performed using standard procedures. Sections were captured using a VisionTek slidescanner (Sakura Americas) at a 10x magnification.

2.6. Sample preparation for ToF-SIMS

Frozen tissue sections were stored at −80 °C. Prior to ToF-SIMS analysis, frozen sections were warmed up to room temperature in a desiccator for 20 min under a vacuum pressure of 20 mbar (SpeedVac, Eppendorf, Hamburg, Germany).

2.7. ToF-SIMS imaging and data analysis

A TOF.SIMS 5 instrument (IONTOF GmbH, Germany) equipped with a bismuth liquid metal ion gun was used. Secondary ion images were acquired in positive mode using Bi_3^{+} primary ions with a pulsed current of 0.1 pA at 25 KeV energy and a maximum ion dose density of 4.91×10^{11} cm^{-2}. The delay extraction mode was used with an extraction voltage of 2 kV, a rise time of 40 ns and a delay of 5 μs. A mass resolution (m/Δm) of 5000 Full Width at Half Maximum (FWHM) was reached at *m/z* 90. Charge effects were limited by electron flooding. Entire tissue sections were imaged in 2D large area scanning mode (settings in Table S1). Close-ups of region of interest were performed in 2D scanning mode with a field of view of 500 × 500 μm divided in 512 × 512 pixels (3 shots per pixel). The lateral resolutions determined with the 16 %-84 % method were 12 μm and 1.8 μm in 2D large area scanning mode and 2D scanning mode, respectively (see Fig. S2).

SurfaceLab 6 software (v. 6.6, ION-TOF GmbH) was used for all spectra and image recording, processing, analysis. The mass spectra were internally calibrated to signals of $[CH_2]^{+}$, $[CH_3]^{+}$, $[Na]^{+}$, $[^{90}Zr]^{+}$ and $[C_5H_{15}PNO_4]^{+}$. All the peaks selected during the data processing are shown in Fig. S4.

3. Results and discussion

To locate Zr-DFO-trastuzumab, the spatial distribution of zirconium was determined by ToF-SIMS imaging. A ToF-SIMS 5 instrument (ION-TOF GmbH, Münster, Germany) equipped with a Bi cluster ion gun was used. The monatomic ions $[^{90}Zr^{+}]$ and $[^{94}Zr^{+}]$ (Fig. S1) were detected in delayed extraction mode with an extraction voltage of 2 kV, a rise time of 40 ns and a delay of 5 μs to reach a mass resolution (m/Δm) of 5000 FWHM at *m/z* 90. A maximum ion dose of Bi_3^{+} of 4.91×10^{11} cm^{-2} was applied to analyse the entire section area by 2D large scan area mapping with an achieved lateral resolution of 12 μm (Fig. S2). Close ups of Zr-rich structures were made in 2D scanning mode by rastering 500 × 500 μm^2 regions divided in 512 × 512 pixels achieving a lateral resolution of 1.8 μm (Fig. S2).

Complementarily, HER2 expression and *in vivo* injected trastuzumab presence were visualized in tissue sections of the same tumour by IHC-staining using a VisionTek slidescanner (Sakura Americas) at a 10x magnification.

Maps of the phosphocholine head group $[C_5H_{15}PO_4N]^{+}$ at *m/z* 184.09 are used to visualize the tissue due to its large abundance (Fig. 3B) [17]. Zirconium is clearly detected in the sections of a $HER2^{+}$ xenograft tumour in a mouse injected with 300 μg of Zr-DFO-trastuzumab (Fig. 3C and D). On the large area scan maps, the Zr

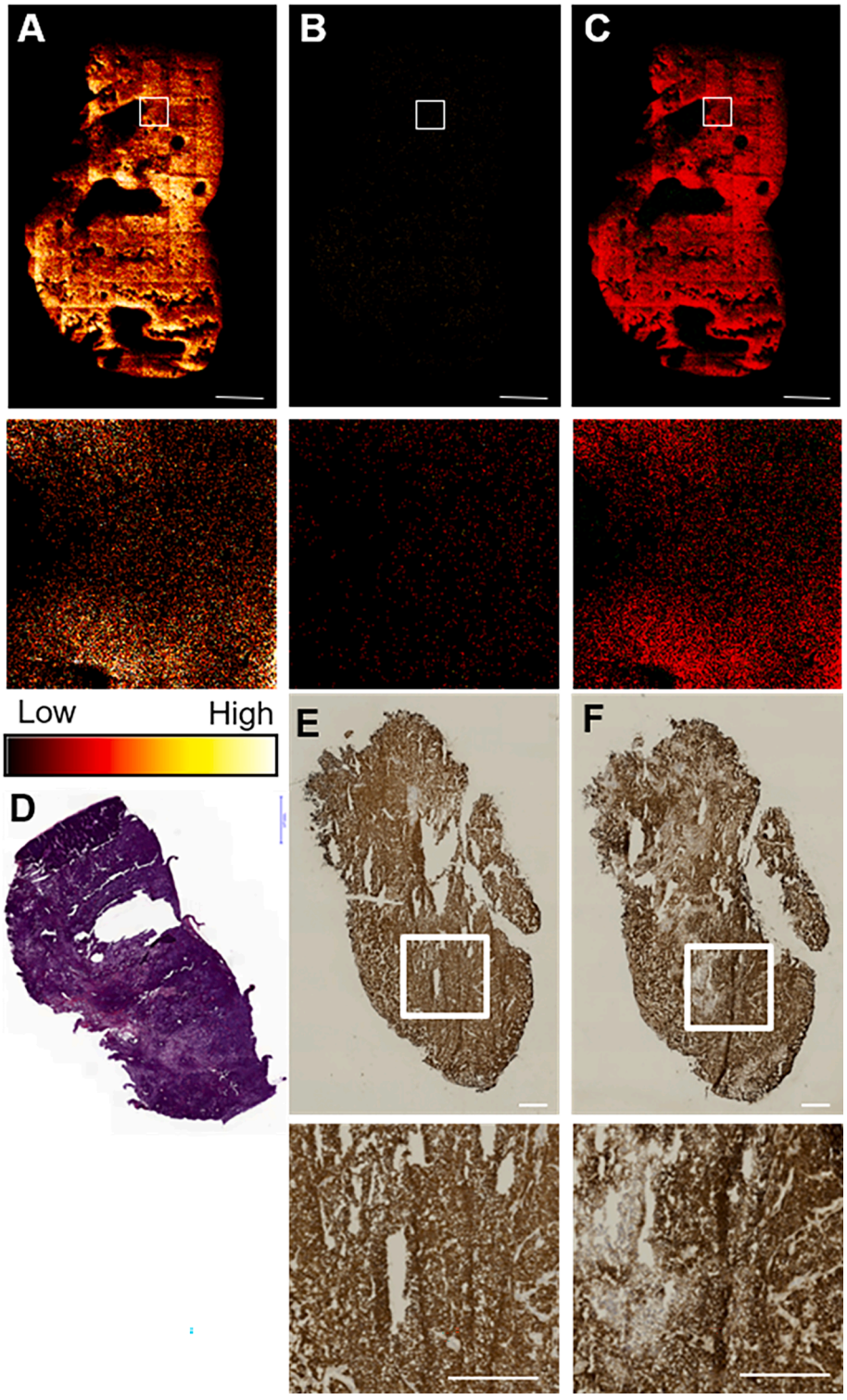

Fig 4. Zirconium spatial distribution in a section of HER2^{+} xenograft tumour in a mouse injected with 300 μg of trastuzumab. (A) TOF-SIMS large scan mapping and corresponding close-up of (A) $[C5H15PO4N]^{+}$ fragment (*m/z* 184.02), (B) $^{90}Zr^{+}$ (*m/z* 89.90) as well as (C) overlay of $[C5H15PO4N]^{+}$ fragment and $^{90}Zr^{+}$ in red and green colour, respectively. Scale bar = 1 mm, close-up field of view = 500x500 μm^2. White arrows show necrosed area. Sections were stained for anatomy observation by haemotoxylin and eosin (D), for HER2 expression (E) and trastuzumab presence (F) with enlargement below the images with the scale bar representing 500 μm. (For interpretation of the references to colour in this figure legend, the reader is referred to the web version of this article.)

spatial distribution seems to be homogeneous in the tissue. However, as shown on the close-ups, some regions of the tissue are richer in zirconium. The size of these areas could correspond to the size of cell clusters where trastuzumab accumulated. The intense staining of trastuzumab by IHC in Fig. 3F demonstrates heterogenous distribution of Zr-DFO-trastuzumab in confirmed HER2 rich tumour tissue (Fig. 3E).

As a control experiment, sections of a HER2^{+} xenograft tumour in a mouse injected with 300 μg of non-labelled trastuzumab were analysed (Fig. 4). Unsurprisingly, the $[^{90}Zr]^{+}$ signal is very low with a signal/noise ratio < 2 and does not allow localization of unlabelled trastuzumab in this sample. However, trastuzumab is confirmed to be present in the tumour at the HER2^{+} areas as indicated by the intense HER2 and trastuzumab staining (Fig. 4 E and F).

Sections of HER2^{-} xenograft tumour in a mouse injected with 300 μg of Zr-DFO-trastuzumab were also analysed. Despite the low HER2 expression determined by HER2 staining (Fig. S3E), ToF-SIMS $[^{90}Zr^{+}]$ ions maps (Fig S3A-D) reveal a heterogeneous distribution of zirconium in the tissue. In the slightly positive HER2 area (Fig. S3E), low uptake of

injected trastuzumab is observed as well (Fig. S3F), which was confirmed by low detection of Zr by ToF-SIMS (Fig. S3B). Low uptake may be explained by binding to the light positive HER2 areas or by non-specific uptake caused by the enhanced permeability and retention (EPR) effect. Low presence of Zr-DFO-trastuzumab in the centre of the section may indicate non-specific uptake in this necrotic tumour area. Such a non-specific uptake of ^{89}Zr-trastuzumab has been demonstrated to be related to non-specific uptake in necrotic areas of xenografts [18]. This is not visible in the HER2^{+} xenograft tumour sections because of the absence of a necrotic area.

4. Conclusions

In conclusion, this study shows for the first time that ToF-SIMS imaging can be used as a quick and sensitive technique to visualize the distribution of zirconium labelled trastuzumab in xenograft tumours. The ToF-SIMS application can be extended to the localization of zirconium labelled biologics in tissue. A complementary analysis by Nanoscale Secondary Ion Mass Spectrometry (NanoSIMS) could provide information regarding fate and effects of immuno-tracers at subcellular level.

CRediT authorship contribution statement

Florent Penen: Investigation, Formal analysis, Writing – original draft. **René Raavé:** Investigation, Writing – review & editing. **Annemarie Kip:** Investigation, Writing – review & editing. **Sandra Heskamp:** Resources, Project administration, Writing – review & editing. **Per Malmberg:** Conceptualization, Resources, Writing – review & editing, Project administration, Funding acquisition, Supervision.

Declaration of Competing Interest

The authors declare that they have no known competing financial interests or personal relationships that could have appeared to influence the work reported in this paper.

Data availability

Data will be made available on request.

Acknowledgements

This study received funding from the Innovative Medicines Initiative 2 Joint Undertaking under grant agreement No 116106. This Joint Undertaking received support from the European Union's Horizon 2020 research and innovation program and EFPIA.

Appendix A. Supplementary data

Supplementary data to this article can be found online at https://doi.org/10.1016/j.microc.2022.107860.

References

[1] S. Heskamp, R. Raavé, O. Boerman, M. Rijpkema, V. Goncalves, F. Denat, 89Zr-immuno-positron emission tomography in oncology: state-of-the-art 89Zr radiochemistry, Bioconjug. Chem. 28 (2017) 2211–2223, https://doi.org/10.1021/acs.bioconjchem.7b00325.

[2] L. Kailas, J.-N. Audinot, H.-N. Migeon, P. Bertrand, ToF-SIMS molecular characterization and nano-SIMS imaging of submicron domain formation at the surface of PS/PMMA blend and copolymer thin films, Appl. Surf. Sci. 231–232 (2004) 289–295, https://doi.org/10.1016/j.apsusc.2004.03.063.

[3] A.M. Kia, N. Haufe, S. Esmaeili, C. Mart, M. Utriainen, R.L. Puurunen, W. Weinreich, ToF-SIMS 3D analysis of thin films deposited in high aspect ratio structures via atomic layer deposition and chemical vapor deposition, Nanomaterials. 9 (7) (2019) 1035.

[4] C.-M. Chan, L.-T. Weng, Y.-T.-R. Lau, Polymer surface structures determined using ToF-SIMS, Rev. Anal. Chem. 33 (2014) 11–30, https://doi.org/10.1515/revac-2013-0015.

[5] B. Joachim, A. Pawley, I.C. Lyon, K. Marquardt (neé Hartmann), T. Henkel, P. L. Clay, L. Ruzié, R. Burgess, C.J. Ballentine, Experimental partitioning of F and Cl between olivine, orthopyroxene and silicate melt at Earth's mantle conditions, Chem. Geol. 416 (2015) 65–78.

[6] A.F.A. Marques, S.D. Scott, R.N.S. Sodhi, Determining major and trace element compositions of exposed melt inclusions in minerals using ToF-SIMS, Surf. Interface Anal. 43 (2011) 436–442, https://doi.org/10.1002/sia.3594.

[7] S. Rinnen, C. Stroth, A. Rißе, C. Ostertag-Henning, H.F. Arlinghaus, Characterization and identification of minerals in rocks by ToF-SIMS and principal component analysis, Appl. Surf. Sci. 349 (2015) 622–628, https://doi.org/10.1016/j.apsusc.2015.04.231.

[8] M.K. Passarelli, A.G. Ewing, N. Winograd, Single-cell lipidomics: characterizing and imaging lipids on the surface of individual Aplysia californica neurons with cluster secondary ion mass spectrometry, Anal. Chem. 85 (2013) 2231–2238, https://doi.org/10.1021/ac303038j.

[9] I. Kaya, S.M. Brülls, J. Dunevall, E. Jennische, S. Lange, J. Mårtensson, A.G. Ewing, P. Malmberg, J.S. Fletcher, On-tissue chemical derivatization of catecholamines using 4-(N-methyl)pyridinium boronic acid for ToF-SIMS and LDI-ToF mass spectrometry imaging, Anal. Chem. 90 (2018) 13580–13590, https://doi.org/10.1021/acs.analchem.8b03746.

[10] S. Fearn, Characterisation of biological material with ToF-SIMS: a review, Mater. Sci. Technol. 31 (2015) 148–161, https://doi.org/10.1179/1743284714Y.0000000668.

[11] K. Wu, F. Jia, W. Zheng, Q. Luo, Y. Zhao, F. Wang, Visualization of metallodrugs in single cells by secondary ion mass spectrometry imaging, JBIC J. Biol. Inorg. Chem. 22 (2017) 653–661, https://doi.org/10.1007/s00775-017-1462-3.

[12] R.F.S. Lee, S. Theiner, A. Meibom, G. Koellensperger, B.K. Keppler, P.J. Dyson, Application of imaging mass spectrometry approaches to facilitate metal-based anticancer drug research, Metallomics. 9 (2017) 365–381, https://doi.org/10.1039/C6MT00231E.

[13] C. Bonechi, M. Consumi, M. Matteucci, G. Tamasi, A. Donati, G. Leone, L. Menichetti, C. Kusmic, C. Rossi, A. Magnani, Distribution of gadolinium in rat heart studied by fast field cycling relaxometry and imaging SIMS, Int. J. Mol. Sci. 20 (2019) 1339, https://doi.org/10.3390/ijms20061339.

[14] J. Malm, D. Giannaras, M.O. Riehle, N. Gadegaard, P. Sjövall, Fixation and drying protocols for the preparation of cell samples for time-of-flight secondary ion mass spectrometry analysis, Anal. Chem. 81 (2009) 7197–7205, https://doi.org/10.1021/ac900636v.

[15] H. Nygren, K. Borner, P. Malmberg, B. Hagenhoff, Localization of cholesterol in rat cerebellum with imaging TOF-SIMS – effect of tissue preparation, Appl. Surf. Sci. 252 (2006) 6975–6981, https://doi.org/10.1016/j.apsusc.2006.02.197.

[16] E.C.F. Dijkers, J.G.W. Kosterink, A.P. Rademaker, L.R. Perk, G.A.M.S. van Dongen, J. Bart, J.R. de Jong, E.G.E. de Vries, M.N. Lub-de Hooge, Development and characterization of clinical-grade ^{89} Zr-trastuzumab for HER2/ *neu* immunoPET imaging, J. Nucl. Med. 50 (2009) 974–981, https://doi.org/10.2967/jnumed.108.060392.

[17] C.R. Anderton, B. Vaezian, K. Lou, J.F. Frisz, M.L. Kraft, Identification of a lipid-related peak set to enhance the interpretation of TOF-SIMS data from model and cellular membranes, Surf. Interface Anal. 44 (2012) 322–333, https://doi.org/10.1002/sia.3806.

[18] J.C. Knight, M.J. Mosley, V. Kersemans, G.M. Dias, P.D. Allen, S. Smart, B. Cornelissen, Dual-isotope imaging allows in vivo immunohistochemistry using radiolabelled antibodies in tumours, Nucl. Med. Biol. 70 (2019) 14–22, https://doi.org/10.1016/j.nucmedbio.2019.01.010.